



# Observation of gas-phase peroxyxynitrous and peroxyxynitric acid during the photolysis of nitrate in acidified frozen solutions

Otman Abida<sup>1</sup>, Levi H. Mielke, Hans D. Osthoff\*

Department of Chemistry, University of Calgary, 2500 University Drive NW, Calgary, Alberta, Canada T2N 1N4

## ARTICLE INFO

### Article history:

Available online 23 June 2011

## ABSTRACT

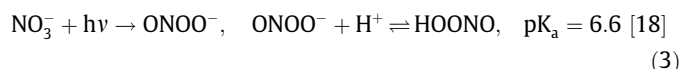
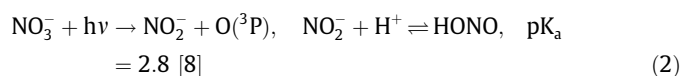
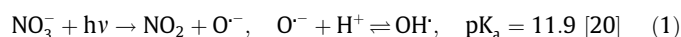
The photolysis of nitrate embedded in ice and snow can be a significant source of volatile nitrogen oxides affecting the composition of the planetary boundary layer. In this work, we examined the nitrogen oxides evolved from irradiated frozen solutions containing nitrate. Products were monitored by cavity ring-down spectroscopy (CRDS), NO-O<sub>3</sub> chemiluminescence (CL), and chemical ionization mass spectrometry (CIMS). Under acidic conditions, the nitrogen oxides volatilized were mainly in the form of NO<sub>x</sub>, i.e., nitrous (HONO), nitric (HONO<sub>2</sub>), peroxyxynitrous (HOONO), and peroxyxynitric acid (HO<sub>2</sub>NO<sub>2</sub>). Identification of acidic nitrogen oxides by CIMS and possible HOONO, HONO<sub>2</sub> and HO<sub>2</sub>NO<sub>2</sub> formation pathways are discussed.

© 2011 Elsevier B.V. All rights reserved.

## 1. Introduction

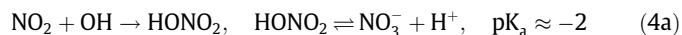
It is well established that photolysis of nitrate anions embedded in snow or ice can be a significant source of gas-phase nitrogen oxides (NO<sub>x</sub> = NO + NO<sub>2</sub>) and hence affect the composition of the planetary boundary layer [1]. Even though the production of volatile nitrogen oxides by this pathway has been the subject of numerous laboratory, field, and theoretical studies (e.g., [2–16]) and of a recent review [17], some mechanistic details have yet to be elucidated. Factors known to affect the yield of gas-phase nitrogen oxides include temperature, presence of organic impurities (e.g., [12,13]), ionic strength, and pH. For example, the rate of NO<sub>x</sub> and HONO production is increased at lower pH (e.g., [9,10]) for reasons that are not fully understood.

Under conditions encountered in the troposphere, ice surfaces are usually covered by a thin liquid layer, referred to as the ‘quasi liquid layer’ (qll). The photochemistry of nitrate in ice is thus similar to that in aqueous solution, for which photolysis of nitrate anion has been shown to produce nitrogen dioxide (NO<sub>2</sub>), nitrite (NO<sub>2</sub><sup>-</sup>), and peroxyxynitrite (ONOO<sup>-</sup>) as primary photoproducts [18,19]; the latter two are protonated under acidic conditions.



NO<sub>2</sub> and HONO are known to partition to the gas-phase [17]. Observations of nitric oxide (NO) have been rationalized by photodissociation of the nitrite anion formed via reaction (2), whose absorption spectrum exhibits greater overlap with the actinic spectrum than nitrate.

Under actinic conditions (i.e., irradiation wavelengths  $\lambda > 300$  nm), the quantum yield for reaction (3) is small [21]. However, recombination of the photo fragments produced in reaction (1) can be an alternate pathway for the photoisomerization of nitrate as reaction (1) is promoted by the so-called ‘solvent cage-effect’ (e.g., [19,22]).



Reaction (4b) can also occur in the gas phase. The latter process is significant since in the lower troposphere HOONO dissociates to form NO<sub>2</sub> and OH [23], key ingredients in photochemical ozone production, whereas nitric acid (HONO<sub>2</sub>), produced via reaction (4a), is generally considered a permanent sink of NO<sub>x</sub>. In polluted environments, the ‘recycling’ of NO<sub>x</sub> via reaction (4b) can have considerable impacts on ozone budgets [24].

Under conditions relevant to the troposphere, HOONO has been a rather elusive molecule. In aqueous solution, both the protonated and deprotonated forms rapidly decompose or isomerize to the more stable nitrate anion [18,25]. In the gas-phase, HOONO is predicted to have a very short lifetime ( $\sim 10$  s) with respect to thermal decomposition at ambient temperature and pressure [23]. As a consequence, HOONO has not been observed in the troposphere

\* Corresponding author. Fax: +1 403 289 9488.

E-mail address: [hosthoff@ucalgary.ca](mailto:hosthoff@ucalgary.ca) (H.D. Osthoff).

<sup>1</sup> Present address: Wadsworth Center, New York State Department of Health, Department of Environmental Health and Toxicology, State University of New York, Albany, NY 12201-0509, USA.

and neither its gas- or liquid-phase lifetime at tropospheric relevant temperatures nor its Henry's law constant are constrained by observations.

Studies on the evolution of volatile nitrogen oxides from irradiated frozen solutions have so far relied on chemiluminescence (CL) detection of NO and of NO<sub>y</sub> (=NO<sub>x</sub> + HONO + HNO<sub>3</sub> + HNO<sub>4</sub>...), on laser-induced fluorescence detection of NO<sub>2</sub> (e.g., [4,5]), and/or on measurement of gas-phase acids using a denuder (also called mist chamber) coupled to ion chromatography (e.g., [14,26]). It is not known if peroxydic and peroxytrioxidic acid would be detected by these techniques or if they are (falsely) accounted for as either NO<sub>2</sub> (in case of LIF) or as nitric acid (in case of the mist chamber) [26].

In this work, we investigated the nature of gas-phase nitrogen oxides evolved from irradiated frozen solutions containing nitrate anion and show that nitric (HNO<sub>3</sub>), nitrous (HONO), peroxydic (HO<sub>2</sub>NO<sub>2</sub>) and peroxytrioxidic (HO<sub>2</sub>NO) acid are volatilized under acidic conditions. We used CL detection to quantify NO and NO<sub>y</sub>, blue diode laser cavity ring-down spectroscopy (CRDS) to measure NO<sub>2</sub>, and iodide ion chemical ionization mass spectrometry (CIMS) to monitor acidic nitrogen oxides.

## 2. Experimental

### 2.1. Ice photolysis experiments

All reagents were analytical grade (>99%) and were used as received. Dilute (0.05 M) buffer solutions were prepared by mixing the appropriate amounts of oxalic acid and sodium oxalate (Sigma–Aldrich, pH 2.5) in de-ionized water (Barnstead EasyPure II; 18 MΩ cm). Aqueous solutions containing up to 1 M sodium nitrate (Sigma–Aldrich, 99%) were prepared immediately prior to the experiments in buffer solution. The pH of the solutions was measured prior to freezing. Oxalic acid was chosen as a buffer as it is usually one of the most abundant species in organic aerosol in the Arctic [27]. The pH chosen is at the lower end of the range typically found in nature. For example, in heavily polluted air, snowflake pH values as low 3.0 have been reported [28].

The photolysis setup is shown in Figure 1. The photolysis light source was a 150 W Xenon arc lamp (ORIEL 'Solar Simulator', model 96000) equipped with an IR filter (ORIEL 81096) and a digital exposure controller (ORIEL 68951). Its output was directed through a cut-off filter window (Pyrex, λ > 300 nm) at the top of reactor. At the maximum power setting, the incident light flux was measured by ferrioxalate actinometry [29] to be 1.5 × 10<sup>16</sup> photons s<sup>-1</sup> cm<sup>-2</sup>. In the experiments shown here, the lamp was operated at lower

power (20 and 40 W). This attenuated the output intensity equally at all wavelengths (data not shown).

The experiments were conducted using a custom-built Pyrex photo reactor (internal volume 275 cm<sup>3</sup>). Samples of frozen solutions were prepared by placing approximately 4 mL of pre-cooled aqueous solution onto the bottom of the photo reactor tube, which was cooled to -20 °C using a circulating chiller (VWR). The reactor was flushed during sample freezing and irradiation with ultrapure, or 'zero', air (Praxair) at a flow rate of (1.4 ± 0.1) L min<sup>-1</sup>. Tubing and compression fittings outside of the photo reactor were constructed from PFA or FEP Teflon. The zero air entered the reaction chamber near the top and exited via a side arm whose opening is located 1 cm above the ice surface, minimizing the residence time of gas-phase products and their contact with the inner walls of the reaction chamber. Upon freezing, polycrystalline ice with an average thickness of about 2 mm and area of approximately 19.6 cm<sup>2</sup> were obtained. The output of the photo reactor was diluted by an additional zero air dilution flow (approximately 8 L/min). The residence time of the effluent within the Teflon tubing connecting the photo reactor to the instruments was <1 s.

### 2.2. Detection and quantification of gas-phase nitrogen oxides

Gas-phase nitrogen oxides were monitored (in parallel) using a commercial NO<sub>y</sub> CL analyzer (Thermo 42i), the University of Calgary blue diode laser CRDS [30], and the University of Calgary I<sup>-</sup>-CIMS [31]. The CRDS uses a blue diode laser to quantify NO<sub>2</sub> by optical absorption at 405 nm. The instrument is equipped with multiple detection channels which allows parallel determination of NO<sub>2</sub> and either total peroxydic (ΣPAN) by thermal dissociation (to NO<sub>2</sub>) at an inlet temperature of 250 °C or total peroxy plus total alkyl nitrates (ΣAN) at an inlet temperature of 450 °C [30,32]. We also used a red diode laser CRDS recently constructed in our laboratory to verify the absence of NO<sub>3</sub> and N<sub>2</sub>O<sub>5</sub>. This instrument is similar to the one described by [33] and will be described in a forthcoming publication [34]. It has a limit of detection (1σ, 10 s) of 5 part-per-trillion by volume (pptv).

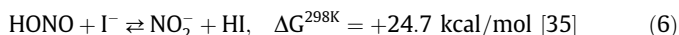
The CL analyzer is equipped with a heated Mo catalyst to reduce the various components of NO<sub>y</sub> to NO and was calibrated against CRDS by simultaneous measurements of NO<sub>2</sub> in zero air and scaling the response of the CL analyzer to that of the CRDS. The conversion efficiency of other NO<sub>y</sub> species (i.e., HONO and HNO<sub>3</sub>) was assumed to be equal to that of NO<sub>2</sub>.

The CIMS and its operation have been described elsewhere [31] with the only difference being that the inlet was operated at room temperature to minimize dissociation of thermally unstable molecules. Iodide reagent ions were generated by passing methyl iodide past a <sup>210</sup>Po ion source. Since the number of ions generated scales with the amount of (excess) iodide reagent ion, all ion counts were normalized to 1 × 10<sup>6</sup> iodide reagent ion counts prior to presentation.

Table 1 summarizes major ions observed when the CIMS is exposed to various nitrogen oxides. Iodide ions react with many nitrogen oxides to form cluster ions (e.g., ClNO<sub>2</sub>·I<sup>-</sup>, N<sub>2</sub>O<sub>5</sub>·I<sup>-</sup>, HONO·I<sup>-</sup>, or HONO<sub>2</sub>·I<sup>-</sup>) which are well-suited for quantification due to low background counts and high specificity. Proton exchange reactions, e.g.,



and



are not thermodynamically favored at room temperature. Reactions of iodide anion with peroxyacids, e.g.,



are well-known from solution phase chemistry (e.g., [36,37]) and can also occur in the gas phase. Hence, The ions NO<sub>2</sub><sup>-</sup> or NO<sub>3</sub><sup>-</sup> are

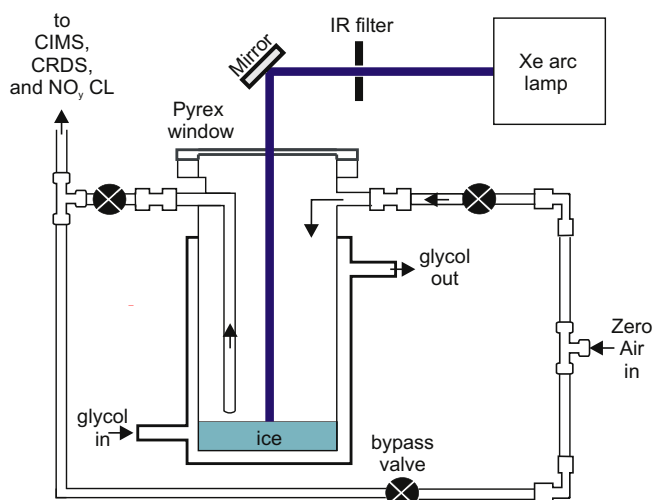


Figure 1. Experimental setup. For a discussion, see Section 2.1 in the text.

**Table 1**  
Detection of nitrogen oxides by iodide ion chemical ionization mass spectrometry.

Species	Major ion ( <i>m/z</i> , rel. intensity)	Ion forming reaction(s)	Minor ion ( <i>m/z</i> , rel. intensity)	Ion forming reaction(s)	Ref.
NO	–	–	–	–	This work
NO <sub>2</sub>	–	–	–	–	This work
NO <sub>3</sub>	62	NO <sub>3</sub> + I <sup>−</sup> → I + NO <sub>3</sub> <sup>−</sup>	–	–	[38]
N <sub>2</sub> O <sub>5</sub>	62 (variable)	N <sub>2</sub> O <sub>5</sub> $\xrightarrow{\Delta}$ NO <sub>3</sub> + NO <sub>2</sub>	235 (variable)	N <sub>2</sub> O <sub>5</sub> + I <sup>−</sup> → N <sub>2</sub> O <sub>5</sub> · I <sup>−</sup>	[39]
		NO <sub>3</sub> + I <sup>−</sup> → I + NO <sub>3</sub> <sup>−</sup>			
ClNO <sub>2</sub>	208 (3)	<sup>35</sup> ClNO <sub>2</sub> + I <sup>−</sup> $\xrightarrow{\text{H}_2\text{O}}$ <sup>35</sup> ClNO <sub>2</sub> · I <sup>−</sup>	210 (1)	<sup>37</sup> ClNO <sub>2</sub> + I <sup>−</sup> $\xrightarrow{\text{H}_2\text{O}}$ <sup>37</sup> ClNO <sub>2</sub> · I <sup>−</sup>	[45]
HONO	174 (8)	HONO + I <sup>−</sup> → HONO · I <sup>−</sup>	46 (1)	HONO + I <sup>−</sup> → HI + NO <sub>2</sub> <sup>−</sup>	This work
HONO <sub>2</sub>	190 (6.6)	HONO <sub>2</sub> + I <sup>−</sup> → HONO <sub>2</sub> · I <sup>−</sup>	62 (1)	HONO <sub>2</sub> + I <sup>−</sup> → HI + NO <sub>3</sub> <sup>−</sup>	This work
HO <sub>2</sub> NO <sub>2</sub>	62 (420)	HO <sub>2</sub> NO <sub>2</sub> + I <sup>−</sup> → HOI + NO <sub>3</sub> <sup>−</sup>	46 (1 <sup>a</sup> )	?	This work
Photo reactor effluent (pH 2.5)	190 (1)	HONO <sub>2</sub> + I <sup>−</sup> → HONO <sub>2</sub> · I <sup>−</sup>	62 (31)	<1%: HONO <sub>2</sub> + I <sup>−</sup> → HI + NO <sub>3</sub> <sup>−</sup>	This work
	174 (1.2)	HONO + I <sup>−</sup> → HONO · I <sup>−</sup>	46 (18)	>99%: HO <sub>2</sub> NO <sub>2</sub> + I <sup>−</sup> → HOI + NO <sub>3</sub> <sup>−</sup>	This work
				<1%: HONO + I <sup>−</sup> → HI + NO <sub>2</sub> <sup>−</sup>	
				>99%: HO <sub>2</sub> NO + I <sup>−</sup> → HOI + NO <sub>2</sub> <sup>−</sup>	

<sup>a</sup> Upper limit.

non-specific since they can arise from proton or electron transfer reactions or fragmentation of other ions.

### 2.3. Generation of gas standards to verify response and determine calibration factors of CIMS

Nitric oxide and nitrogen dioxide were generated by diluting the output of an NO cylinder (Praxair, 2.28 ppm NO in N<sub>2</sub>, certified) and periodically adding ozone (generated by photolysis of oxygen using a Hg pen ray lamp) to partially oxidize NO to NO<sub>2</sub>. No elevated ion counts were observed by CIMS in either case. Addition of stoichiometric amounts of ozone generated a response at *m/z* 62, interpreted as arising from NO<sub>3</sub> or N<sub>2</sub>O<sub>5</sub> [38,39]. We note that neither NO, NO<sub>2</sub>, nor NO<sub>3</sub>/N<sub>2</sub>O<sub>5</sub> produced a signal at *m/z* 46 (NO<sub>2</sub><sup>−</sup>).

Gas-phase nitric and nitrous acid were eluted from passive diffusion sources containing either concentrated nitric acid or a concentrated solution of sodium nitrite and measured in parallel by CIMS and CL. For HONO<sub>2</sub>, the major ion observed was at *m/z* 190 due to the iodide cluster ion, with a normalized response factor of 1.2 counts per pptv. Ion counts were also observed at *m/z* 62 due to fragmentation with an intensity of 1:6 relative to the cluster ion. For HONO, the major ion observed was HONO · I<sup>−</sup> at *m/z* 174 with a normalized response factor of 0.14 counts pptv<sup>−1</sup>. The fragment ion, at *m/z* 46, had an intensity of 1:8 relative to *m/z* 174.

Peroxyntoxic acid was synthesized using the method described in Ref. [40] and sampled using a passive diffusion source yielding mass counts at only *m/z* 62. Since the synthesis method did not yield a pure sample and *m/z* 62 is not specific to HO<sub>2</sub>NO<sub>2</sub>, a response factor was not determined; judging from the parallel CL measurements, the response factor is orders of magnitudes higher than that of HONO at *m/z* 174 or HONO<sub>2</sub> at *m/z* 190.

We also attempted to synthesize gas-phase HO<sub>2</sub>NO. The synthetic route used was inspired by [41] and involved passing a gas stream containing HONO over an aqueous solution containing 50% H<sub>2</sub>O<sub>2</sub>. The resulting mass spectrum (not shown) contained peaks at *m/z* 190, 174, 62 and 46. The presence of *m/z* 46 can be rationalized by a reaction analogous to reaction (7):



## 3. Results

### 3.1. Production of gas-phase nitrogen oxides

Photolysis of nitrate anion in either unbuffered or basic frozen solutions yielded NO<sub>2</sub> as the major (>90%) gas-phase nitrogen

oxide (data not shown). Photolysis of nitrate in acidified frozen solutions yielded a greater amount of gas-phase nitrogen oxides (NO<sub>y</sub>), with the major fraction in the form of NO<sub>z</sub> (=NO<sub>y</sub>–NO<sub>x</sub>). For example, the top panel of Figure 2 shows a time series of NO, NO<sub>2</sub> and NO<sub>y</sub> emitted from an irradiated frozen sample containing 1.0 M nitrate and 0.05 M oxalate buffer (pH 2.5). In this experiment, the lamp was switched on at 10:35 local time at a power setting of 20 W, switched off briefly at 11:02, and switched on again at 11:06 at a power setting of 40 W. When the lamp was turned off, the NO<sub>2</sub> signal rapidly returned to baseline. The response of the CL analyzer was slower, signifying the presence of one or more ‘sticky’ NO<sub>y</sub> component(s). When the lamp power was increased, the amount of NO<sub>2</sub> and NO<sub>y</sub> evolved also increased.

The middle panel of Figure 2 shows the CIMS mass counts observed at *m/z* 62 and 190, respectively. The ratio of the ion counts observed at *m/z* 62 relative to *m/z* 190 (31:1) far exceeded the amount expected if only HONO<sub>2</sub> were present (*m/z* 62:190 ≈ 1:6.6; Table 1 and Figure 3). Furthermore, the responses at *m/z* 62 and 190 were not well correlated (Figure 2), in particular during period 1, i.e., from 10:40 to 10:50. Thus, different molecules were contributing to each of these mass counts. Species that could contribute to *m/z* 62 (other than HONO<sub>2</sub>) are NO<sub>3</sub>, N<sub>2</sub>O<sub>5</sub> [38], PANs [31], and HO<sub>2</sub>NO<sub>2</sub> (Table 1). We briefly operated the CIMS with a heated inlet [31,38] and verified the absence of PANs. Using the red diode laser CRDS, we verified that neither NO<sub>3</sub> nor N<sub>2</sub>O<sub>5</sub> were formed in the experiment. Thus, the most plausible explanation is that the counts at *m/z* 62 were mainly due to HO<sub>2</sub>NO<sub>2</sub>, consistent with the results with the synthetic standard.

The response at both masses was delayed relative to the modulation of the lamp intensity, and was sustained for some time after the lamp was turned off. This suggests that these mass counts arise from a ‘sticky’ compound, i.e., compounds whose sorption and desorption kinetics on the inner walls of the connecting tubing is slow (HONO<sub>2</sub> at *m/z* 190), or that these compounds continued to outgas from the ice surface ‘in the dark’ (HO<sub>2</sub>NO<sub>2</sub> at *m/z* 62).

The bottom panel shows the corresponding time series at *m/z* 46 and 174. The response at both masses to lamp intensity changes was more rapid than for *m/z* 62 and 190. The counts at *m/z* 46 are correlated with the amount of NO<sub>2</sub> observed by CRDS (*r*<sup>2</sup> = 0.89). Since NO<sub>2</sub> does not give a signal at *m/z* 46, the ratio of ion counts (Figure 3) at *m/z* 46 relative to *m/z* 174 is more than 100× greater than observed for HONO, and the mass spectrometer’s ion chemistry promotes conversion of peroxyacids to anions (Eqs. (7) and (8)), we conclude that the high counts at *m/z* 46 are mainly due to HOONO.

We considered that matrix effects may be affecting the ratio of the cluster ions at *m/z* 174 and 190 relative to the fragment ions at

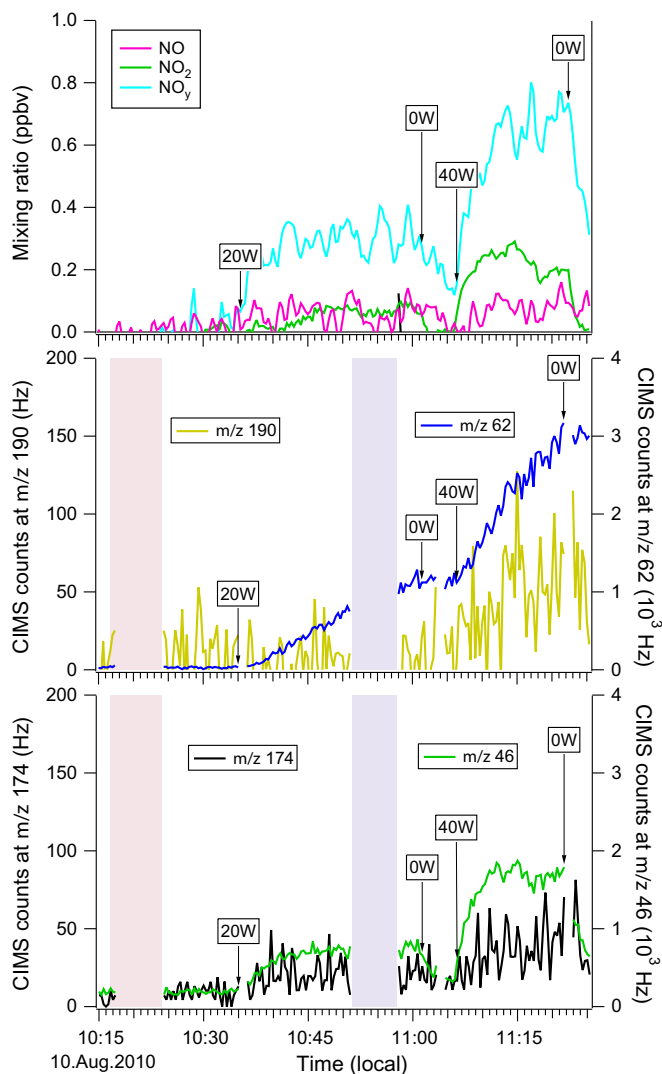


**Figure 2.** Production of gas-phase nitrogen oxides from an irradiated frozen solution containing 1.0 M nitrate anion and 0.05 M oxalate buffer (pH 2.5). (top) Time series of NO, NO<sub>2</sub>, and NO<sub>y</sub> mixing ratios. The power levels indicated are those of the Xe arc lamp. (middle) Time series of *m/z* 190 (HONO<sub>2</sub>I<sup>-</sup>) and *m/z* 62 (NO<sub>3</sub><sup>-</sup>) for the same experiment. The pale red and blue underlays are the times during which mass spectra (Figure 3) were acquired. (bottom) Time series of *m/z* 174 (HONO<sub>2</sub>I<sup>-</sup>) and *m/z* 46 (NO<sub>2</sub><sup>-</sup>) for the same experiment. (For interpretation of the references in color in this figure legend, the reader is referred to the web version of this article.)

*m/z* 46 and 62. To verify the absence of such effects, standard addition experiments were carried out in which the effluent of the photo reactor was mixed with either nitrous or nitric acid. The ion ratios observed (not shown) were identical to those in the off-line experiment shown in Figure 3, corroborating that the ion counts at *m/z* 46 and 62 are mainly due to molecules other than nitrous or nitric acid.

Using the calibration factors for HONO<sub>2</sub> at *m/z* 190 and for HONO at *m/z* 174, the fractionation of NO<sub>y</sub> was calculated (Table 2). For period 2, the major NO<sub>y</sub> species evolved are HONO (35% relative to measured NO<sub>y</sub>), NO<sub>2</sub> (33%), NO (12%) and HONO<sub>2</sub> (6%). The sum of these nitrogen oxides, ΣNO<sub>y (cold)</sub>, accounts for 86% of the observed NO<sub>y</sub>. The amount of NO<sub>2</sub> observed in the heated CRDS channel is slightly greater than that observed in the room temperature channel (data not shown), approximately 47% relative to NO<sub>y</sub> observed. The difference between the 'hot' and 'cold' CRDS channel observed is approximately 13% (relative to NO<sub>y</sub>). Because NO<sub>3</sub>, N<sub>2</sub>O<sub>5</sub>, and PANs were absent, the difference signal was likely due to peroxy nitrates. If the amount of NO<sub>2</sub> observed in the 'hot' CRDS

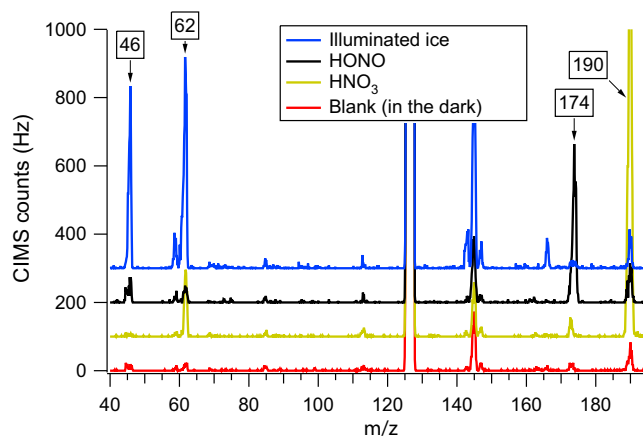


**Figure 3.** CIMS mass spectra, offset in increments of 100 counts for clarity. The bottom (red) trace and the top (blue) scans were taken during the time periods indicated in Figure 2. The scans offset by 100 and 200 counts (gold and black, respectively) are reference mass spectra of HONO<sub>2</sub> and HONO, respectively. (For interpretation of the references in color in this figure legend, the reader is referred to the web version of this article.)

channel is included, the sum of nitrogen oxides, ΣNO<sub>y (hot)</sub>, equals 101% of the observed NO<sub>y</sub> (Table 2).

### 3.2. Radical quenching experiments

To gain insight into the mechanism for HO<sub>2</sub>NO and HO<sub>2</sub>NO<sub>2</sub> formation, radical quenching experiments were carried out in which either hexane was periodically added to the zero air entering the photolysis chamber or 0.02 M isopropanol was added to the solutions prior to freezing. The presence of isopropanol reduced the overall yield of nitrogen oxides without affecting the fractionation of NO<sub>y</sub>. The addition of hexane to the gas-phase had no statistically relevant effect on NO<sub>y</sub>.

## 4. Discussion

### 4.1. Acid-promoted production of HONO(g) and NO(g)

Under acidified conditions, photolysis of nitrate produced a considerable amount of gas-phase NO<sub>2</sub> species. The observed formation of HONO is consistent with previous reports (e.g., [6,12,15,16]) and can be rationalized as follows: Photolysis of nitrate anion is known to produce nitrite (reaction 2), which in acidic medium is protonated and partitions to the gas-phase (Henry's law constant at room temperature = 49 M atm<sup>-1</sup> [42]). Beine and coworkers have reported positive fluxes of nitrous acid under acidic conditions [16], while under basic conditions, emission of nitrous acid was found to be suppressed [15]. The experiment here demonstrates acid-promoted release of HONO to the gas-phase. Subsequent photolysis of nitrous acid, whose absorption spectrum has a greater overlap with the lamp's emission spectrum than nitrate, yields NO (as observed).

### 4.2. Acid-promoted production of HONO<sub>2</sub>(g), HO<sub>2</sub>NO<sub>2</sub>(g), and HO<sub>2</sub>NO(g)

The data provide strong evidence that nitrogen oxides other than NO, NO<sub>2</sub> and HONO are emitted by the irradiated ice. It is certain that HONO<sub>2</sub> is generated. It is unlikely that HONO<sub>2</sub> forms in the ice and is then volatilized because its pK<sub>a</sub> is approximately -2, i.e., deprotonation to the nonvolatile nitrate anion is strongly favored in ice, and because its Henry's law constant for water at room temperature is large (~10<sup>5</sup> M atm<sup>-1</sup> [42]). Hence, it is more

**Table 2**Yields of NO<sub>y</sub> species (in ppbv) for the experiment shown in Figure 2. The uncertainties are ±1σ, i.e., indicate the precision of the measurements.

Species	Period 1 (10:40–10:50)	±	Period 2 (11:13–11:18)	±	Percentage rel. to NO <sub>y</sub> (obs) (%)
NO	0.06	0.04	0.08	0.03	12
NO <sub>2</sub> (cold CRDS inlet)	0.05	0.03	0.22	0.04	33
NO <sub>2</sub> + (heated CRDS inlet)	0.10	0.04	0.32	0.07	47
HONO	0.09	0.07	0.24	0.11	35
HONO <sub>2</sub>	–0.01	0.01	0.04	0.02	6
∑NO <sub>y</sub> (cold CRDS inlet)	0.19		0.58		86
∑NO <sub>y</sub> (heated CRDS inlet)	0.24		0.68		101
NO <sub>y</sub> (obs)	0.29	0.05	0.67	0.07	–

likely that gas-phase HONO<sub>2</sub> is produced by a secondary process, e.g., by reaction (4a). It is unclear if reaction (4a) occurs in the gas phase, either in the tubing connecting the reactor to the CIMS or just above the ice surface, or in the condensed phase (i.e., within the qll), even though the latter two are more likely since addition of hexane to the zero air had no obvious effect on the production of nitrogen oxides and addition of isopropanol lowered the yield of nitrogen oxides.

If reaction (4a) is used to rationalize production of HONO<sub>2</sub>, it implies that NO<sub>2</sub> and OH are there in abundance. Thus, reaction (4b) should also occur and HOONO should be produced. This is consistent with the observation of very high ion counts at *m/z* 46, assigned to HOONO. One interesting feature of the counts at *m/z* 46 is that they respond rapidly to changing light intensity, unlike those at the other nitrogen oxide masses observed by CIMS. This is, at first, surprising, since one might expect relatively slow sorption and desorption kinetics on the inner walls of the connecting tubing. However, since HOONO is thermally unstable, it is unlikely that slow desorption kinetics from the inner walls will give rise to inlet memory effects or a sustained background signal.

#### 4.2.1. Proposed mechanism for formation of HOONO and HONO<sub>2</sub>

Since the quantum yield for HOONO formation from nitrate photolysis is small in the actinic region [21], HOONO is most likely formed by reaction (4b), i.e., recombination of the nitrate photo products, O<sup>–</sup> (which rapidly protonates to OH) and NO<sub>2</sub>. This reaction is likely promoted by the solvent cage. Since HOONO's pK<sub>a</sub> is 6.6 [18], the protonated form will dominate at pH 2.5. The Henry's law constant for the partitioning of HOONO between the ice and gas phase is not known; however, it is reasonable to assume that the Henry's law constant of HOONO is more similar to that of HONO than of HONO<sub>2</sub>. Considering that the rate of thermal decomposition and isomerization of HOONO in ice is likely slower in ice at –20 °C than in solution at room temperature, it is plausible that HOONO is sufficiently long-lived to at least partially partition to the gas-phase.

Once partitioned to the gas-phase, the fate of HOONO is thermal decomposition. This would have 'masked' HOONO formation in previous experiments; we can observe HOONO mainly because of the rapid analysis time (<1 s) used. The decomposition products, OH and NO<sub>2</sub>, can combine to HONO<sub>2</sub> (reaction (4a)) or recombine to form HOONO (reaction (4b)); however, since OH is efficiently 'lost' (e.g., by wall reactions), a considerable fraction of the emitted HOONO will end up as NO<sub>2</sub>. Hence, volatilization of HOONO is one of the mechanisms by which NO<sub>2</sub> is volatilized from the ice surface. This mechanism would be consistent with observations by Honrath et al. [14] and others, who have noted that the presence of OH radical quenchers in the ice suppresses the yield of NO<sub>2</sub>.

#### 4.2.2. Proposed mechanism for formation of HO<sub>2</sub>NO<sub>2</sub>

The most likely HO<sub>2</sub>NO<sub>2</sub> formation pathway is from reaction of NO<sub>2</sub> with HO<sub>2</sub> within the qll:



Peroxyntiric acid has a pK<sub>a</sub> of 5.85 [43], and will be present mainly in the protonated form under the conditions of the experiment. Its Henry's law constant for room temperature solutions is approximately 10<sup>4</sup> M atm<sup>–1</sup> [36]. Considering that volatilization of HONO<sub>2</sub> was observed whose Henry's law constant is one order of magnitude larger, it is not surprising that volatilization of HO<sub>2</sub>NO<sub>2</sub> is also observed.

The source of HO<sub>2</sub> is somewhat uncertain. It is known that oxalate in the presence of Fe<sup>3+</sup> produces superoxide (O<sub>2</sub><sup>–</sup>) [29]. The hydroperoxyl radical has a pK<sub>a</sub> of approximately 4.8 [44]; thus, HO<sub>2</sub> could be produced from protonation of O<sub>2</sub><sup>–</sup>. However, Fe<sup>3+</sup> is present at most in trace quantities (arising from impurities in the chemical reagents); hence, we expect this pathway to be negligible. Another potential HO<sub>2</sub> source is photolysis of ONOO<sup>–</sup> [25]. Since ONOO<sup>–</sup> is rapidly protonated at pH 2.5, we speculate that HO<sub>2</sub> is a product of HOONO photolysis.

Peroxyntiric acid is thermally unstable. It is hence interesting to observe that the response to changes in lamp power of *m/z* 62 is slower than of *m/z* 46, which suggests either that HO<sub>2</sub>NO<sub>2</sub> slowly desorbs from the inner walls of the Teflon tubing, outgasses from the ice surface 'in the dark', or both.

## 5. Conclusions

This work demonstrates that HONO<sub>2</sub>, HOONO and HO<sub>2</sub>NO<sub>2</sub> can be formed as volatile secondary products following photolysis of nitrate anion in acidic ice and that these molecules can be observed by mass spectrometry. The release of these nitrogen oxides is not currently considered in mechanisms describing the photochemical transformation of nitrate in snow (e.g., [9]); however, the results presented here suggest that this pathway could be significant. Further work, including measurements of the yields of nitrogen oxides in intermediate pH ranges and at lower nitrate concentrations, will be needed to assess the importance of this chemistry in the troposphere.

## Acknowledgments

We gratefully acknowledge financial support by the Canadian Foundation for Climate and Atmospheric Sciences (CFCAS) under Grant No. GR-7054 and funding from the Alberta Ingenuity Fund in the form of a New Faculty Award. The CIMS used in this work was purchased using a National Science and Engineering Research Council (NSERC) Research Tools and Instruments (RTI) Grant.

## References

- [1] R.E. Honrath, M.C. Peterson, S. Guo, J.E. Dibb, P.B. Shepson, B. Campbell, *Geophys. Res. Lett.* 26 (1999) 695.
- [2] L. Chu, C. Anastasio, *J. Phys. Chem. A* 107 (2003) 9594.
- [3] Y. Dubowski, A.J. Colussi, M.R. Hoffmann, *J. Phys. Chem. A* 105 (2001) 4928.
- [4] C.S. Boxe, A.J. Colussi, M.R. Hoffmann, J.G. Murphy, P.J. Wooldridge, T.H. Bertram, R.C. Cohen, *J. Phys. Chem. A* 109 (2005) 8520.

- [5] C.S. Boxe, A.J. Colussi, M.R. Hoffmann, I.M. Perez, J.G. Murphy, R.C. Cohen, J. Phys. Chem. A 110 (2006) 3578.
- [6] H.J. Beine, A. Amoroso, F. Dominé, M.D. King, M. Nardino, A. Ianniello, J.L. France, Atmos. Chem. Phys. 6 (2006) 2569.
- [7] H.J. Beine, F. Domine, A. Ianniello, M. Nardino, I. Allegrini, K. Teinila, R. Hillamo, Atmos. Chem. Phys. 3 (2003) 335.
- [8] C. Anastasio, L. Chu, Environ. Sci. Technol. 43 (2009) 1108.
- [9] H.W. Jacobi, B. Hilker, J. Photochem. Photobiol. A-Chem. 185 (2007) 371.
- [10] C.S. Boxe, A. Saiz-Lopez, Atmos. Chem. Phys. 8 (2008) 4855.
- [11] J.L. Thomas, M. Roeselova, L.X. Dang, D.J. Tobias, J. Phys. Chem. A 111 (2007) 3091.
- [12] T. Bartels-Rausch et al., Atmos. Environ. 44 (2010) 5443.
- [13] C. George, R.S. Strekowski, J. Kleffmann, K. Stemmler, M. Ammann, Faraday Discuss. 130 (2005) 195.
- [14] R.E. Honrath, S. Guo, M.C. Peterson, M.P. Dziobak, J.E. Dibb, M.A. Arsenaault, J. Geophys. Res.-Atmos. 105 (2000) 24183.
- [15] H.J. Beine et al., Geophys. Res. Lett. 32 (2005) L10808.
- [16] X.L. Zhou, H.J. Beine, R.E. Honrath, J.D. Fuentes, W. Simpson, P.B. Shepson, J.W. Bottenheim, Geophys. Res. Lett. 28 (2001) 4087.
- [17] A.M. Grannas et al., Atmos. Chem. Phys. 7 (2007) 4329.
- [18] J. Mack, J.R. Bolton, J. Photochem. Photobiol., A 128 (1999) 1.
- [19] G. Mark, H.-G. Korth, H.-P. Schuchmann, C. von Sonntag, J. Photochem. Photobiol., A 101 (1996) 89.
- [20] G.V. Buxton, C.L. Greenstock, W.P. Helman, A.B. Ross, J. Phys. Chem. Ref. Data 17 (1988) 513.
- [21] S. Goldstein, J. Rabani, J. Am. Chem. Soc. 129 (2007) 10597.
- [22] T.G. Koch, J.R. Sodeau, J. Phys. Chem. 99 (1995) 10824.
- [23] D.M. Golden, J.R. Barker, L.L. Lohr, J. Phys. Chem. A 107 (2003) 11057.
- [24] A.K. Mollner et al., Science 330 (2010) 646.
- [25] R. Kissner, T. Nauser, P. Bugnon, P.G. Lye, W.H. Koppenol, Chem. Res. Toxicol. 10 (1997) 1285.
- [26] R.W. Talbot, A.S. Vijgen, R.C. Harriss, J. Geophys. Res.-Atmos. 95 (1990) 7553.
- [27] K. Kawamura, H. Kasukabe, L.A. Barrie, Atmos. Environ. 30 (1996) 1709.
- [28] J.L. Colin, D. Renard, V. Lescoat, J.L. Jaffrezou, J.M. Gros, B. Strauss, Atmos. Environ. 23 (1989) 1487.
- [29] J.G. Calvert, J.N. Pitts, Photochemistry, Wiley, New York, 1966.
- [30] D. Paul, H.D. Osthoff, Anal. Chem. 82 (2010) 6695.
- [31] A. Furgeson, L.H. Mielke, D. Paul, H.D. Osthoff, Atmospheric Environment 45 (2011). doi:10.1016/j.atmosenv.2011.03.072.
- [32] D. Paul, A. Furgeson, H.D. Osthoff, Rev. Sci. Instrum. 80 (2009) 114101. doi:10.1063/1.3258204.
- [33] W.R. Simpson, Rev. Sci. Instrum. 74 (2003) 3442.
- [34] C.A. Odame-Ankrah, H.D. Osthoff, Applied Spectroscopy (2011) submitted (June 15), manuscript i.d. 11-06384.
- [35] J.E. Bartmess, in: P.J. Linstrom, W.G. Mallard (eds.), National Institute of Standards and Technology, Gaithersburg, MD, 2011, <<http://webbook.nist.gov>> (retrieved 16.06.11).
- [36] J.-M. Régimbal, M. Mozurkewich, The Journal of Physical Chemistry A 101 (1997) 8822.
- [37] J.-M. Régimbal, M. Mozurkewich, The Journal of Physical Chemistry A 104 (2000) 6580.
- [38] D.L. Slusher, L.G. Huey, D.J. Tanner, F.M. Flocke, J.M. Roberts, J. Geophys. Res.-Atmos. 109 (2004) D19315. doi:10.1029/2004JD004670.
- [39] J.P. Kercher, T.P. Riedel, J.A. Thornton, Atmos. Meas. Tech. 2 (2009) 193.
- [40] E.H. Appelman, D.J. Gosztoła, Inorg. Chem. 34 (1995) 787.
- [41] K.M. Robinson, J.S. Beckman, Nitric Oxide, Pt E, 2005. pp. 207–214.
- [42] S.E. Schwartz, W.H. White, in: J.R.Z. Pfafflin (Ed.), Advances in Environmental Science and Engineering, Gordon and Breach Science Publishers, NY, 1981, pp. 1–45.
- [43] T. Loegager, K. Sehested, J. Phys. Chem. 97 (1993) 10047.
- [44] B.H.J. Bielski, D.E. Cabelli, R.L. Arudi, A.B. Ross, J. Phys. Chem. Ref. Data 14 (1985) 1041.
- [45] H.D. Osthoff et al., Nat. Geosci. 1 (2008) 324.